Erik Stein*, Rongqing Chen, Alberto Battistel, and Knut Moeller

Separating Respiration and Perfusion in EIT: Harmonic Analysis on 2D-Thorax Simulation

https://doi.org/10.1515/cdbme-2022-1200

Abstract: Electrical impedance tomography (EIT) has the potential for monitoring perfusion in addition to respiration on the bedside. Several separation methods were reported, e.g. Filtering, ECG-gating and PCA. However, the separation is not trivial, which is why harmonic analysis was introduced in EIT data analysis. It is based on several assumptions and therefore prove of plausibility is necessary. In this contribution a two-dimensional thorax simulation is introduced, which includes simplified lungs and heart with changing shapes and conductivities due to volume variations and lung perfusion. Harmonic analysis was applied on the simulated data. The separation results are in good agreement with the simulation settings. Further investigations will be required due to limitations of the simulation. Nevertheless, harmonic analysis delivered precise results in ideal and strictly defined conditions.

Keywords: Electrical impedance tomography, harmonic analysis, separation of respiration and perfusion, simulation

1 Introduction

Electrical Impedance Tomography (EIT) is a non-invasive, radiation-free imaging technique, which reveals impedance changes within an investigated area by applying alternating currents with an electrode belt [1, 2].

Currently, EIT is mostly applied for bedside ventilation monitoring of mechanically ventilated patients [1, 2], but regional lung perfusion is not monitored. Actually, perfusion is equally as important as ventilation for gas exchange in the alveoli. The ventilation/perfusion-ratio (V/Q-ratio) should be close to one [3], to ensure a successful ventilation support.

Respiration and perfusion signals are both included in EIT measurements and, as Putensen et al. [4] suggested, these signals could be used for gaining information about the V/Q-ratio. This could, eventually, enhance guidance of mechanical ventilation [2]. To obtain the information of mismatch, the signal components of respiration and perfusion need to be separated, which is challenging [2, 4, 5]: Firstly, signals related to perfusion are significantly weaker in amplitude than those of respiration [6]. Secondly, their frequency bands can be in superposition because higher harmonics of respiration overlap into the region of the basis heart frequency [5]. Thirdly, it is still not completely understood what causes perfusion related impedance changes [4, 7].

Several separation approaches have been developed, e.g. digital filtering, ECG-gating, bolus injection of contrast agents, apnea and principal component analysis (PCA) [4]. Especially digital filtering and ECG-gating have significant disadvantages [4]. Filtering is not suitable when the frequency spectra of respiration overlaps that of perfusion; while ECG-gating is time delayed due to averaging processes and needs additional measurements [4]. Apnea is not suitable in severe patients if measurements are repeated over a long time.

Battistel et al. [5] proposed a novel approach, implementing the harmonic analysis on EIT measurements. Harmonic analysis is applicable on overlapping frequency bands and does not require additional monitoring tools. However, the approach depends on five assumptions: Respiration and perfusion are expressible as sums of amplitude modulated signals, they are stable over time regarding their frequencies, they are smooth enough to be reconstructed as low order polynomials, they do not share harmonics, and lung perfusion and cardiac activity share the same frequency.

In this contribution we aim to prove the plausibility of the harmonic analysis method. A two dimensional simulation model was built containing a simplified heart and two simplified lungs. Harmonic analysis was applied on the simulated data.

2 Methods

2.1 EIT

Being an ill-posed inverse problem, EIT has significantly less measurement values $\mathbf{y}$ available than are necessary for a precise reconstruction $\hat{\mathbf{x}}$ of the internal properties $\mathbf{x}$ [1]. In difference EIT, where voltage measurements $\mathbf{v}$ are related to a reference $\mathbf{v_r}$, measurements values are defined as $\mathbf{y} = \mathbf{v} - \mathbf{v_r}$ and internal tissue properties as changes in conductivity $\mathbf{x} = \boldsymbol{\sigma} - \boldsymbol{\sigma_r}$ [1]. The reconstructed internal properties, i.e. conduc-

***Corresponding author: Erik Stein,** Institute of Technical Medicine, Furtwangen University, Jakob-Kienzle-Str. 17, VS-Schwenningen, Germany, e-mail: erik.stein@hs-furtwangen.de
Rongqing Chen, Alberto Battistel, Knut Moeller, Institute of Technical Medicine, Furtwangen University, VS-Schwenningen, Germany

tivity differences, are calculated by

$$\hat{\mathbf{x}} = (\mathbf{J}^t\mathbf{W}\mathbf{J} + \lambda^2\mathbf{R})^{-1}\mathbf{J}^t\mathbf{W}\mathbf{y} = \mathbf{B}\mathbf{y} \quad (1)$$

where $\mathbf{J}$ is the sensitivity matrix, which maps measurement sensitivities to conductivity changes [1]. The identity matrix $\mathbf{W}$ represents the reliability of each measurement channel and a hyperparameter λ controls the weight of the regularization matrix $\mathbf{R}$, which contains prior knowledge [1]. $\mathbf{B}$ is the resulting reconstruction matrix [1].

2.2 Harmonic Analysis

Harmonic analysis is described in detail by Battistel et al. [5], but in general can be written as

$$\hat{y}(t) = \sum_{p=0}^{N_p}\sum_{n=1}^{N_h}(\hat{\theta}^g_{nf,p}\cos(2\pi nft) - \hat{\theta}^h_{nf,p}\sin(2\pi ft))b_p(t) \quad (2)$$

where a reconstructed signal $\hat{y}$, is expressed as the sum of in-phase and out-of-phase modulated signals with coefficients $\hat{\theta}$ obtained in a least square sense, which control a set of basis functions $b_p(t)$. In this method the basis functions are hermite polynomials. N_h describes the number of harmonics which are fitted and N_p the number of coefficients that are used for fitting. The frequency f is either the basis heart or respiration rate resulting in two separated signals $\hat{y}_r$ and $\hat{y}_p$.

The coefficients are determined by fitting the harmonics and intermodulations of respiration and perfusion with hermite functions in the frequency domain. The first six harmonics of respiration and the first two of perfusion were considered in this analysis. The fitting can be conducted on global and pixel-wise impedance values, resulting in an overall and pixel specific separation of respiration and perfusion.

Parameters need to be set to specify how many coefficients per frequency should be used for fitting. For perfusion related frequencies, five coefficients were used and two for all others, i.e. respiration and intermodulations. The width of the gaussian window, which lets hermite functions decay when approaching infinity, was set to two.

Because hermite functions are eigenvectors of the fourier transform, the calculated coefficients from the frequency domain can be used for reconstructing respiration and perfusion separately with hermite polynomials in the time domain.

2.3 Simulation

Matlab R2019b (Mathworks, Natick, MA) and the EIDORS toolbox (Version 3.10) [8] were used for simulation. The finite element model (FEM) was generated with NETGEN (Version 5.3) [9], which is integrated into EIDORS.

Tab. 1: Different tissue conductivities for AC frequencies of 100 kHz [10]

Tissue	Conductivity [$\mathrm{S \cdot m^{-1}}$]
Blood	0.70
Heart Muscle	0.22
Lung (Deflated)	0.27
Lung (Inflated)	0.11
Fat	0.04
Muscle	0.36

The shapes of lung and heart were modelled with ideal circular areas, which differ in radius and location in a thoracic-shaped two-dimensional FEM. Radius changes were calculated in dependence of cylindrical volume changes, which were based on cosine functions.

In simulation, the volume of each lung over time ($V_L(t)$) was calculated as

$$V_L(t) = \frac{1}{2}(V_{FRC} + \frac{V_T}{2}\cos(2\pi f_R t) + \frac{V_T}{2}) \quad (3)$$

where V_T is the tidal volume. It is reported to be 500 ml in healthy adults [3]. V_{FRC} is the functional residual capacity (FRC) and describes the amount of air remaining in the lungs during normal breathing, which is about three liters [3].

In simulation, the myocardial volume over time ($V_M(t)$) was calculated by

$$V_M(t) = V_{M_{max}} - \frac{1}{2}(V_S\cos(2\pi f_H t) + V_S) \quad (4)$$

where $V_{M_{max}}$ is the maximum heart volume, including the myocardium, and was assumed to be 360 ml [11]. The change in volume is described by V_S and equals the biventricular stroke volume, which is about 140 ml [11].

One blood chamber was added in the hearts center. It represents the two ventricles, which, in reality, beat synchronously with similar stroke volumes. The chambers volume over time $V_C(t)$ is calculated as

$$V_C(t) = V_{EDV} - \frac{1}{2}(V_S\cos(2\pi f_H t) + V_S) \quad (5)$$

where V_{EDV} is an end-diastolic volume of 240 ml [3]. V_S is the same stroke volume as in equation 4.

f_R and f_H describe the frequencies of respiration and heart activity, which were chosen to be 0.25 Hz and 1.17 Hz respectively.

For an alternating current frequency of 100 kHz [1] the different tissue conductivities used in the simulation are listed in Table 1 [10]. The background conductivity was set to 0.2 $\mathrm{S \cdot m^{-1}}$ and calculated as the average between fat and muscle conductivity. The heart was modeled as a heart muscle surrounding one large ventricle filled with blood. The change in lung tissue conductivity $\sigma_{L_L}(t)$ was modeled as

$$\sigma_{L_L}(t) = \frac{\sigma_{def} + \sigma_{inf}}{2} - \frac{\sigma_{def} - \sigma_{inf}}{2}\cos(2\pi f_R t) \quad (6)$$

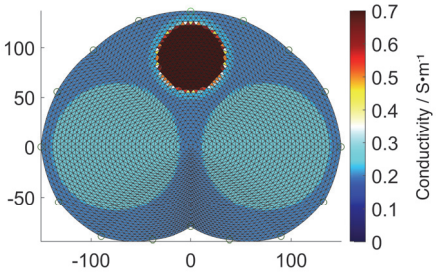

Fig. 1: Lungs (light green) and heart (dark red) in thoracic shaped FEM-mesh with their specific conductivities at time 3 s

where σ_{def} and σ_{inf} are the lung tissue conductivities at maximum expiration and maximum inspiration, respectively.

In this simulation the lung perfusion $\sigma_{L_B}(t)$ was assumed to be linearly related to changes in blood volume in the pulmonary system and is described as

$$\sigma_{L_B}(t) = \sigma_B - \frac{0.14 \cdot \sigma_B}{2} \cos(2\pi f_H t - \pi) \qquad (7)$$

where σ_B is the blood conductivity. After each heartbeat 35 ml of blood are pumped into each lung and each lung carries about 250 ml of blood (V_{pul}), which results in a blood volume change of 14% per heartbeat [3]. The change in conductivity ($\sigma_{L_B}(t)$) was calculated according to this percentage with an additional phase-shift of 180° in relation to heart activity [4]. The lung conductivity $\sigma_L(t)$ is calculated by

$$\sigma_L(t) = \frac{\sigma_{L_L}(t) \cdot V_L(t) + \sigma_{L_B}(t) \cdot V_{pul}}{V_L(t) + V_{pul}} \qquad (8)$$

where lung tissue $\sigma_{L_L}(t)$ and lung perfusion $\sigma_{L_B}(t)$ conductivities are combined by averaging. The average was weighted with their volume proportions.

The FEM with assigned conductivities is illustrated in Figure 1. Simulated measurements were conducted with adjacent stimulation pattern. The reference voltages for difference imaging were measured at time 6 s. Reconstruction was performed with the one step Gauss-Newton algorithm and Laplace prior with a hyperparameter λ of 0.1. No artificial noise was added to the simulation data.

3 Results and Discussion

In Figure 2 the frequency spectrum of the global impedance is presented and the respiration and cardiac harmonics are clearly visible. The separation results are depicted in Figure 3 and show good overlap with their simulation settings.

The respiration related impedance changes correlate closely to inspiration and expiration, but are steeper when decreasing and flatter when increasing. This is caused by the interaction between changes in lung tissue conductivity $\sigma_{L_L}(t)$

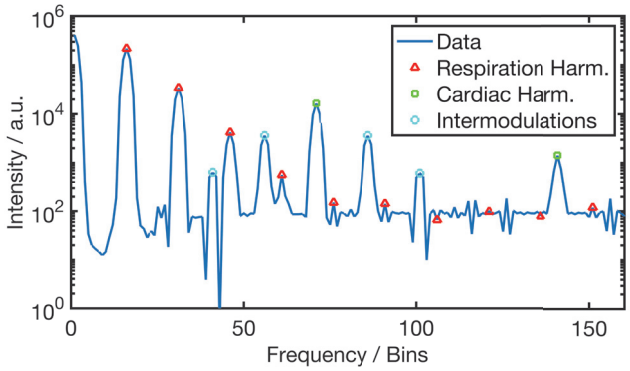

Fig. 2: Plot of global impedance with harmonics and intermodulations in frequency domain

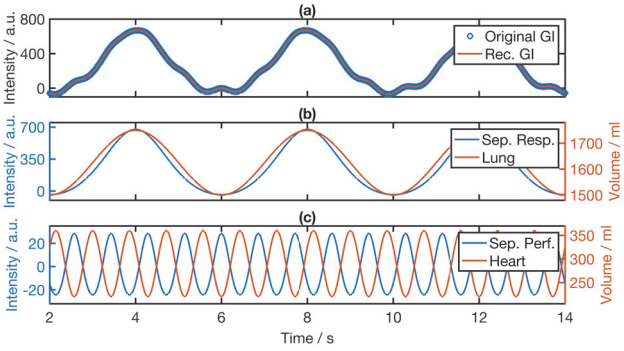

Fig. 3: Comparison of reconstructed global impedance (a), separated respiration (b) and perfusion (c) with their simulation model counterparts global impedance (a), lung (b) and heart volume (c)

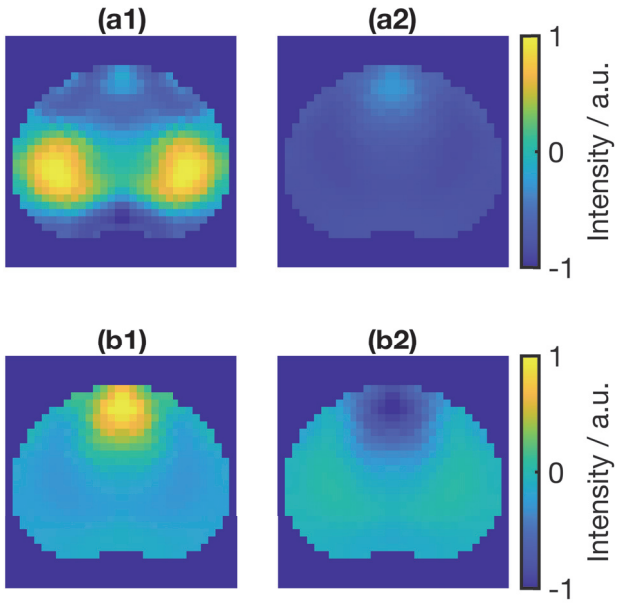

Fig. 4: Respiration (a1 max. inspiration, a2 max. expiration) and perfusion (b1 end-systolic, b2 end-diastolic) related images after pixel-wise separation with harmonic analysis

and lung volume $V_L(t)$. Figure 4 depicts the pixel-wise separation, where end of inspiration and expiration are well visible in (a1) and (a2) respectively. The pixel intensities in Figure 4 were rescaled to [-1,1].

For perfusion, shown in Figure 3, heart volume and impedance correlate negatively. When the heart volume increases, the perfusion related impedance decreases. This matches the expected result because with an increase in heart volume more conductive blood is present in the modeled chamber and consequentially impedance decreases. Lung perfusion is not visible in the graph (Figure 3) because it has a 180° phase shift to heart activity according to equation 7 and is probably too weak in amplitude to make an observable difference. Nevertheless, lung perfusion is well visible in Figure 4 (b2) and changes accordingly during the cardiac cycle.

However, our research has limitations. The model is two-dimensional, the lungs are perfectly symmetrical and the heart only consists of one large ventricle surrounded by myocardium and is placed in the middle of the thorax. Volume changes are based on pure cosine functions and therefore disregard time differences between inspiration and expiration and between systole and diastole as well. The myocardial conductivity is modelled as isotropic, but in reality is highly anisotropic and should therefore be dependent on measurement direction [4]. Additionally, lung perfusion in the simulation is simplified, as that blood related conductivity changes have a linear relationship to changes in blood volume. Also, only pulsatile volume changes were modeled for simulating perfusion, disregarding other sources [7]. Lastly, the background conductivity was simply calculated as an average of fat and muscle conductivity and skeletal structures were not present at all.

Nevertheless, this simplified simulation allowed us to make comparisons between the original and separated signals related to respiration and perfusion, without overlapping too many possible signal origins and loosing the ability to distinguish them.

4 Conclusion

Perfusion monitoring in EIT has not reached clinical use yet, which could mostly be caused by the lack off sufficient separation algorithms and especially their validation. In this contribution, harmonic analysis is shown to be capable of delivering precise results in ideal and strictly defined conditions. However, the simulation model bares limitations and consequentially, further investigations will be required.

Author Statement

Research funding: This research was partially supported by the German Federal Ministry of Education and Research (MOVE, Grant 13FH628IX6) and H2020 MSCA Rise (#872488 DCPM). Conflict of interest: Authors state no conflict of interest. Informed consent: Not applicable. Ethical approval: The conducted research is not related to either human or animal use.

References

[1] Andy Adler and Alistair Boyle. “Electrical Impedance Tomography: Tissue Properties to Image Measures.” In: *IEEE transactions on bio-medical engineering* 64.11 (2017), pp. 2494–2504. DOI: 10.1109/TBME.2017.2728323.

[2] Inéz Frerichs et al. “Chest electrical impedance tomography examination, data analysis, terminology, clinical use and recommendations: consensus statement of the TRanslational EIT developmeNt stuDy group.” In: *Thorax* 72.1 (2017), pp. 83–93. DOI: 10.1136/thoraxjnl-2016-208357.

[3] Stefan Silbernagl and Andreas Draguhn. *Taschenatlas Physiologie*. 9. vollständig überarbeitete Auflage. Stuttgart: Thieme, 2018. ISBN: 978-3-13-241030-5.

[4] Christian Putensen et al. “Electrical Impedance Tomography for Cardio-Pulmonary Monitoring.” In: *Journal of clinical medicine* 8.8 (2019). ISSN: 2077-0383. DOI: 10.3390/jcm8081176.

[5] Alberto Battistel et al. “Harmonic Analysis for the Separation of Perfusion and Respiration in Electrical Impedance Tomography.” In: *IFAC-PapersOnLine* 54.15 (2021), pp. 281–286. ISSN: 24058963. DOI: 10.1016/j.ifacol.2021.10.269.

[6] J. M. Deibele, H. Luepschen, and S. Leonhardt. “Dynamic separation of pulmonary and cardiac changes in electrical impedance tomography.” In: *Physiological measurement* 29.6 (2008), pp. 1–14. ISSN: 0967-3334. DOI: 10.1088/0967-3334/29/6/S01.

[7] Andy Adler et al. “Origins of Cardiosynchronous Signals in EIT.” In: *Proceedings of the 18th International Conference on Biomedical Applications of Electrical Impedance Tomography* (2017), p. 73. DOI: 10.5281/zenodo.557093.

[8] Andy Adler and William R. B. Lionheart. “Uses and abuses of EIDORS: an extensible software base for EIT.” In: *Physiological measurement* 27.5 (2006), pp. 25–42. ISSN: 0967-3334. DOI: 10.1088/0967-3334/27/5/S03.

[9] Joachim Schöberl. “NETGEN An advancing front 2D/3D-mesh generator based on abstract rules.” In: *Computing and Visualization in Science* 1.1 (1997), pp. 41–52. ISSN: 1432-9360. DOI: 10.1007/s007910050004.

[10] Hasgall PA et al. *IT’IS Database for thermal and electromagnetic parameters of biological tissues*. 2022. DOI: 10.13099/VIP21000-04-1. URL: https://itis.swiss/virtual-population/tissue-properties/ (visited on 04/04/2022).

[11] Johann S. Schwegler and Runhild Lucius. *Der Mensch: Anatomie und Physiologie*. 6., überarbeitete Auflage. CNE Bibliothek. Stuttgart and New York: Georg Thieme Verlag, 2016. ISBN: 978-3-13-100156-6.